Title:

Verification of beam delivery using fibrosis after proton beam irradiation to the lung tumor

Nobuyoshi Fukumitsu, Yoshiko Oshiro, Takayuki Hashimoto, Toshiyuki Okumura, Masashi Mizumoto, Takashi Moritake, Koji Tsuboi, Takeji Sakae, Hideyuki Sakurai

Proton Medical Research Center, University of Tsukuba, Tsukuba, Japan.

Reprint requests:

Nobuyoshi Fukumitsu, M.D.

Proton Medical Research Center, University of Tsukuba,

1-1-1, Tennoudai, Tsukuba, 305-8575, Japan.

TEL: 81-29-853-7100

FAX: 81-29-853-7102

Email: fukumitsun@yahoo.co.jp

Abstract

Background and Purpose: To investigate the geometrical accuracy in proton beam therapy (PBT) to the lung by comparing the location of the fibrosis after PBT and the tumor using less invasive method.

Patients and Methods: We examined 50 lung tumors that had been treated by respiratory-gated PBT (33 – 74 Gray equivalents). Image registration and re-slicing of computed tomography (CT) before and after PBT were performed using an image analysis software system. We investigated whether the location of fibrosis was accurate with the tumor site and which factor among the respiratory rhythm, tumor volume, location, fixation, beam direction and clinical outcome was affected with accuracy.

Results: The area of fibrosis was accurate with the tumor in 45 tumors (Group A) and not accurate in 5 tumors (Group B). All lesions with a small irregularity of respiratory rhythm showed fibrosis in an area accurate with

the tumor. This percentage (100%) was higher than that of the lesions with a large irregularity of respiratory rhythm (67%, p=0.037). Radiation pneumonitis was found for 1 lesion in group A and 2 lesions in group B (p=0.0009).

Conclusion: The geometrical accuracy of beam delivery to the lung was higher in the patients with a regular respiratory rhythm in PBT. The patients of group B had greater risk of pneumonitis.

Key words: proton beam therapy, lung tumor, respiratory-gated therapy, fibrosis, CT, geometrical accuracy

Introduction

To increase the precision of radiotherapy, reducing geometric uncertainties, induced by interfraction setup variations and intrafraction breathing movements, is essential as these can lead to differences between the planned dose distribution and the actually delivered radiation dose.

A variety of methods have been reported for monitoring the interfraction setup variation, including the isocenter dose reproducibility [1], repeated radiographs [2], and repeated CT examinations [3]. A variety of methods have also been reported for monitoring intrafraction breathing movements, including electronic portal images [2], fluoroscopy [4], tumor movement from CT [5], dose-volume histograms [6], and the calculation of the geometric error based on respiratory motion data [7]. Moreover, not only interfraction setup variations and intrafraction breathing movements can alter the dose distribution, but also the changes in Hounsfield units

(HU) during breathing [8], mechanical response delays [7], and tumor volume changes during the treatment course. Hence, the accuracy of the dose delivery is too complex to be confirmed or predicted based solely on an evaluation of the setup or breathing-related movements of the lung tumor. To our knowledge, a radiographic investigation of the geometric accuracy of irradiation to lung tumors using an image registration technique has not been previously reported.

Fibrosis on CT images occur following lung irradiation. In proton beam therapy (PBT), the proton beam allows a rapidly increasing dose at the end of the beam range [9]. PBT is clinically used in some kind of tumor treatment utilizing its physical and biological characteristics [10-13]. Excellent dose localization of the proton beam causes a localized fibrosis in and surrounding the tumor after irradiation. Images obtained after radiotherapy show the final effect after all factors affecting geometric

accuracy have been applied. Thus, the fibrosis has potential to evaluate real geometrical accuracy that is not achievable by investigating individual factors.

The aim of this study was to investigate the accuracy of proton beam delivery and depth to the lung by examining the locations of fibrosis and the tumor using an image analysis software system.

Material and Methods

We analyzed data for 50 lung tumor lesions from 48 patients (median: 69.5 years old [range, 46 – 84 years]; 36 men, 12 women) who underwent PBT between January 2004 and June 2010 at the University of Tsukuba and were followed up with a chest computed tomography (CT) examination after PBT. The diagnosis was lung cancer in 41 lesions, metastatic lung tumor in 8 lesions, and plasmacytoma in 1 lesion.

The selection criteria included lesions with a constant irradiation field and any field size or beam direction that was not changed during the course of treatment. Lesions with mild to moderate fibrosis (slight homogeneous increase in radiographic density or patchy consolidation) on follow-up chest CT examinations were selected and lesions with undetectable fibrosis, severe fibrosis (confluent consolidation) or severe distortion of the lung field arising from large quantities of pleural effusion or adhesions on follow-up chest CT examinations were excluded because image comparisons in such cases were thought to be unreliable.

A treatment planning CT examination was performed one week before PBT. The chest CT scan was performed using a respiratory-gated acquisition protocol. The respiratory waveform was obtained from a laser displacement sensor (LDS) that could be focused on an area around the patient’s navel. A gate signal was given to enable exposure once the

respiratory waveform dropped below a certain threshold. The start of exposure was triggered by the gate signal at the end of exhalation phase (Figure 1). To achieve this gating, the CT table was moved to the next slice position after scanning. All the slices (5 mm thick) were scanned downwards from the top of the diaphragm. The pitch was 5 mm.

The clinical target volume (CTV) was contoured as the gross tumor volume (GTV) plus a 5 – 10-mm margin on serial CT images. An additional 5-mm margin in the inferior direction was added to the CTV as an internal margin for respiratory movement. The planning target volume was defined as an internal target volume plus a 5 – 10-mm margin (5 mm: 7 lesions, 7 mm: 12 lesions, 8 mm: 14 lesions, 10 mm: 17 lesions) in all directions.

Proton beams of 155 – 250 MeV were generated using a synchrotron accelerator at the Proton Medical Research Center, University

of Tsukuba. The beams were delivered under respiratory gating through one to four ports using a rotational gantry. During each treatment session, the position was examined using an orthogonal fluoroscopy unit attached to the treatment unit. The dose distribution was calculated using a pencil beam algorithm. The beam delivery devices were selected automatically by the treatment-planning system. A collimator was produced using a brass array. A range-compensating bolus was fabricated with a tissue-equivalent material. The beam delivery system created a homogeneous dose distribution at the prescription dose using the spread-out Bragg peak of the proton beams. The irradiation dose was 33 – 74 (median: 66) Gray equivalent (GyE) over 8 – 35 fractions. The fractionation varied according to the tumor location and the general condition of the patient.

A chest CT examination for diagnosis was performed within 1 month before and 4 – 20 (median: 12) months after PBT (CT [pre], CT

[post], respectively). The chest CT scans were obtained using a breath-hold acquisition protocol. A slice thickness of 5 mm with a slice interval of 5 mm was used.

The image analysis was performed using the Dr. View/LINUX image analysis software system (AJS Inc., Tokyo, Japan).

We performed image registration of the CT (post) image using the CT (pre) image as a reference, both were obtained using a breath-hold acquisition protocol. For the image registration, we set 7 matching points (tracheal bifurcation, bifurcation of bilateral main bronchi, upper and lower thoracic spine, and bilateral sternoclavicular joints) on both the CT (pre) and CT (post) images for image registration. Next, we used a three-dimensional rigid registration using marker fitting and the least squares method; in this manner, the CT (post) image was

three-dimensionally registered and re-sliced at the same position relative to the CT (pre) image.

We investigated accuracy of the fibrosis and the tumor. We defined accurate as fibrosis of re-sliced CT (post) overlap at least partially with the tumor of CT (pre) in their fusion image and not accurate as normal lung field aeration found between fibrosis and the tumor in all slice. We then examined the relevance of fibrosis-tumor accuracy and the respiratory rhythm, tumor volume, location, fixation, beam direction and clinical outcome.

Data analysis and statistics

Firstly, we examined the ratio that location of fibrosis in CT (post) was accurate or not with the tumor in CT (pre). We used lung window in CT (pre) to delineate the tumor. CT (pre) which was performed using a

breath-hold acquisition protocol was different from treatment planning CT performed using a respiratory-gated acquisition protocol. However, tumor delineation in CT (pre) almost corresponds to GTV in the treatment planning CT. Each lesion was classified according to whether the fibrosis was accurate (Group A) or not accurate (Group B) with the actual tumor. Lesions for which the fibrosis was accurate at least partially with the tumor were included in Group A, and only lesions for which the fibrosis was not completely overlapped with the tumor and normal lung field aeration was found between fibrosis and the tumor were included in Group B.

Next, we investigated the relevance of the respiratory rhythm, tumor volume, tumor location, tumor fixation, and beam direction on the ratio of tumor and fibrosis accuracy. In the analysis of the respiratory rhythm, we randomly selected respiratory waveforms during 25 proton beam exposures and measured each beam cycle as the interval from one

beam to the next beam (Figure 1). The value of 25 set of beam cycle was converted into the percent normalization and then we calculated the 90% confidence intervals of the percent normalization of the beam cycle (90% B.C.) as a scale for respiratory rhythm irregularity. The tumor volume was classified as large and small, based on the CTV. The tumor location was classified as upper or lower, with the major fissure as the boundary line. The tumor fixation was classified as fixed to or free from a rigid structure, such as the aorta, vertebra, or chest wall. Finally, the beam direction was classified as anterior or posterior according to the most prominent side of dose delivery. The Fisher exact probability test was used to compare the significance of the ratios of tumor and fibrosis accuracy to the classification of the 90% B.C., tumor volume, tumor location, tumor fixation and beam direction. We decided on cut-off values that was clear-cut and enabled

well-balanced numbers of patients in the classifications for 90% B.C. and tumor volume.

Finally, we investigated the relevance of clinical follow-up data on the tumor and fibrosis accuracy. The local control rate and probability of radiation pneumonitis with a severity of more than Grade 3 (Radiation Therapy Oncology Group's radiation morbidity scoring criteria) [14] as calculated using the Kaplan-Meier method, and a log-rank test was performed to compare Group A and B. A value of $p < 0.05$ was considered significant.

Results

Group A contained 45 lesions, while Group B contained 5. In Group B, the fibrosis was located in antero-medial, postero-caudal, medial,

medial-cranial, and medial-caudal directions from the tumor, respectively. All 5 patients of group B was received 66GyE.

The value of the 90% B.C. was calculated for 25 lesions that were evaluated after the start of respiratory data recording (August 2006). The median value of the 90% B.C. was 21.8% (range, 1.7 – 63.8%) for all the lesions. Among the 16 lesions with a 90% B.C$\leq$ 25%, all the lesions were classified in group A, while among the 9 lesions with a 90% B.C. > 25%, 6 lesions were classified in group A and 3 lesions were classified in group B (p=0.037, Table 1).

Twenty-eight lesions were located in the upper lobe of the lung, while 22 lesions were located in the lower lobe. Ten lesions were fixed to a rigid structure, and 40 lesions were free from the surrounding structures. The median CTV was 18.1 cm^3 (range, 2 – 445 cm^3) for all the lesions. Twenty-seven lesions had a volume$\leq$ 20 cm^3, and 23 had a volume > 20

cm^3. The beam direction was predominantly anterior for the treatment of 15 lesions and predominantly posterior for the treatment of 16 lesions. The remaining 19 lesions were irradiated equally from the anterior and posterior. No significant difference in the tumor location, tumor fixation, tumor volume, or beam direction was found between the two groups (Table 1).

In group A, local recurrences were found for 5 lesions at 3, 11, 12, 24 and 28 months after irradiation, respectively (median observation period for group A, 25 months [range, 3 – 80 months]), and the local control rate was 84.3% at 5 years. In group B, a local recurrence was found for 1 lesion at 16 months after irradiation (median observation period for Group B, 48 months [range, 7 – 83 months]), and the local control rate was 75.0% at 5 years. No significant difference in the local control rates was observed between the two groups (p=0.646). In Group A, one lesion was associated with Grade 3 pneumonitis at 1 month, yielding an event

probability rate of 2.2% at 3 years. In Group B, two lesions were associated with Grade 3 pneumonitis at 5 and 6 months, respectively, yielding an event probability rate of 40% at 3 years. The event probability rate was significantly higher in Group B (p=0.0009).

In a limited analysis of 41 lung cancer lesions, local recurrences were found for 4 lesions at 11, 12, 24 and 28 months after irradiation, respectively (median observation period for group A, 26 months [range, 4 – 80 months]), and the local control rate was 84.0% at 5 years. In group B, a local recurrence was not found after irradiation (median observation period for Group B, 60 months [range, 48 – 83 months]). No significant difference in the local control rates was observed between the two groups (p=0.477).

Figures 2 and 3 shows the CT (pre), registered CT (post), and dose distribution images for representative lesions in Groups A and B, respectively.

Discussion

This study evaluated whether an adequate irradiation dose was actually delivered to the tumor based on the fibrosis in the lung field. To the best of our knowledge, this is the first study to investigate the accuracy of the actual proton beam delivery in a non-invasive manner in the lung.

As shown in the present results, patients with a large 90% B.C. had an increased risk of geometric error. In our system, the proton beam delivery is required for 0.3 seconds after the respiratory waveform drops below a threshold value and proton beam is delivered at most 0.3 seconds. However, the proton beam is not always delivered during a constant respiratory phase. In particular, irregular dropping of the respiratory waveform below the threshold can vary the phase of the proton beam delivery and the beam cycle. Moreover, some patients do not have an

adequate respiratory rhythm for respiratory-gated irradiation. Respiratory movement affects the target volume difference and the dose convolution, and patients with an irregular respiratory rhythm have a risk of geometrical inaccuracy during radiotherapy [7, 15]. In our previous study examining liver tumor patients, the 90% B.C. value was the only factor that determined the geometrical accuracy [16]. We used the same cut-off value (25%) in the present study for the reason the value is close to the mean value and adequate for group classification. The results of this study were quite similar and reproducible, compared with the results of liver tumor patients. Despite the popularity of respiratory-gated radiotherapy, geometrical errors may still occur in patients with an extremely irregular respiratory rhythm. Taken together, these results show that a large variation in the beam cycle causes geometric uncertainties, and lung tumor patients with extremely irregular respiratory rhythms should be encouraged to

perform regular respiration. Some kinds of device have been developed for regulation of respiratory rhythm. The education of patients with regard to achieving a stable and suitable respiratory rhythm could increase the geometrical dose delivery. The patients who have difficulty to perform regulation of respiratory rhythm should be treated using a larger margin or an alternative technique. Tumor movement and variations in tumor movement are known to be much larger in the superior-inferior direction than in the anterior-posterior or left-right directions [6, 17, 18]. In this study, no obvious trend was found in the locations of the fibrosis and the tumors, partly because of the small number of lesions in Group B. All patients of Group B was received 66 GyE as mentioned in Results section. In this study, most of patients (58%) received 66 GyE, followed by 72.6 GyE (22%) and only patients who showed radiation fibrosis were selected.

Thus, investigation of radiation dose affecting severity or detectability of fibrosis by CT was not performed.

The lung exhibits respiratory-induced flexibility, and lung tumors move differently, depending upon their location. Using fluoroscopy, Seppenwoolde et al. clearly demonstrated that tumors located in the lower lobe without attachment to a rigid structure moved with a large motion amplitude (12 ± 2 mm) in the cranial-caudal direction [17]. Minohara et al. reported interesting data indicating that the water-equivalent path length of the posterior side varied to a much larger extent than that of anterior side during the respiratory cycle, and this variation led to uncertainties in the range end of the particle beam [8]. In the present study, however, the geometric accuracy of the proton beam delivery and depth was unaffected by the tumor volume, location, fixation, or beam direction.

As shown in the results, no significant difference in the local control rate was found between the lesions in group A and those in group B. The reason for this finding is difficult to explain for small sample size of group B. Diverse pathology and stage further make complication of data interpretation. However, in our previous study, the local control rate was 97.0% at 2 years in patients with stage I non-small-cell lung cancer [19], and 11.4% of the patients with stage II or stage III non-small-cell lung cancer developed local recurrences during a median 16-month observation period [20]. This high local control rate may make it difficult to draw a definitive conclusion.

As shown in the probability of event results, the lesions in Group B were associated with a high risk of radiation pneumonitis. It is hard to explain the reason. The tumor volumes of the two lesions associated with radiation pneumonitis in Group B were not very large (35 and 9.1 cm^3,

respectively). In respiratory function, both patients exhibited mild restrictive ventilatory impairment (%VC=77.2 and 71.4%, respectively). We suspect that some kind of underlying disease in the lung, such as lung fibrosis, may have caused the irregular respiratory rhythm, and a larger number of patients with an underlying disease that caused irregular respiratory rhythm have been included in Group B. However, limited number of events has limitation of detailed comparative study. Further investigation of a larger number of patients is needed to elucidate this point.

In recent years, an autoactivation study examined the geometrical accuracy in PBT [21]. This autoactivation study is probably the only published method of verifying the area of proton beam irradiation visually. This method produces a clear and easily understandable image. However, because the images of activated ^{11}C that is mainly activated after proton

beam irradiation are made using a PET camera, an expensive capital investment is needed. Moreover, because the half-life of ^{11}C is only 20 min, it is not suitable for verifying irradiation using multi-ports. In addition, the image resolution of PET images is not necessarily suitable for verifying the accuracy of irradiation. We compared CT before and after PBT using rigid registration technique. Rigid registration is simple and widely used technique. In spite of fibrosis and tumor shrinkage cause deformity of lung field, the deformity was quite small because we selected the image of approximate 1 year after treatment and excluded the case with large deformity. We consider that the presently reported method comparing the the actual tumor's location and the fibrosis after irradiation using CT and an image registration technique may be useful for solving these problems.

Conclusion

Large variation in beam intervals cause geometric uncertainties, and patients with extremely irregular respiratory rhythms might require education regarding respiration or should be treated using a larger margin or an alternative technique.

Acknowledgements

This research is (partly) supported by the “Funding Program for World-Leading Innovative R&D on Science and Technology (FIRST Program),” initiated by the Council for Science and Technology Policy (CSTP).

Conflict of Interest Statement

Non declared.

References

1. Piermattei A, Cilla S, Grimaldi L, Viola P, Frattarolo L, D'Onofrio G, Craus M, Fidanzio A, Azario L, Greco F, Digesu C, Deodato F, Macchia G, Morganti AG. Real time transit dosimetry for the breath-hold radiotherapy technique: an initial experience. Acta Oncol 2008;47: 1414-1421.

2. Wong J, Yan D, Michalski J, Graham M, Halverson K, Harms W, Purdy J. The cumulative verification image analysis tool for offline evaluation of portal images. Int J Radiat Oncol Biol Phys 1995;33: 1301-1310.

3. Eccles C, Brock KK, Bissonnette JP, Hawkins M, Dawson LA. Reproducibility of liver position using active breathing coordinator for liver cancer radiotherapy. Int J Radiat Oncol Biol Phys 2006;64: 751-759.

4. Ford EC, Mageras GS, Yorke E, Rosenzweig KE, Wagman R, Ling CC. Evaluation of respiratory movement during gated radiotherapy using film and electronic portal imaging. Int J Radiat Oncol Biol Phys 2002;52: 522-531.

5. Patel AA, Wolfgang JA, Niemierko A, Hong TS, Yock T, Choi NC. Implications of respiratory motion as measured by four-dimensional computed tomography for radiation treatment planning of esophageal cancer. Int J Radiat Oncol Biol Phys 2009;74: 290-296.

6. Langner UW, Keall PJ. Accuracy in the localization of thoracic and abdominal tumors using respiratory displacement, velocity, and phase. Med Phys 2009;36: 386-393.

7. Vedam S, Docef A, Fix M, Murphy M, Keall P. Dosimetric impact of geometric errors due to respiratory motion prediction on dynamic multileaf collimator-based four-dimensional radiation delivery. Med

Phys 2005;32: 1607-1620.

8. Minohara S, Endo M, Kanai T, Kato H, Tsujii H. Estimating uncertainties of the geometrical range of particle radiotherapy during respiration. Int J Radiat Oncol Biol Phys 2003;56: 121-125.

9. Suit H, Urie M. Proton beams in radiation therapy. J Natl Cancer Inst 1992;84: 155-164.

10. Mizumoto M, Sugahara S, Nakayama H, Hashii H, Nakahara A, Terashima H, Okumura T, Tsuboi K, Tokuuye K, Sakurai H. Clinical results of proton-beam therapy for locoregionally advanced esophageal cancer. Strahlentherapie und Onkologie : Organ der Deutschen Rontgengesellschaft ... [et al] 2010;186: 482-488.

11. Mizumoto M, Nakayama H, Tokita M, Sugahara S, Hashii H, Sakae T, Tsuboi K, Sakurai H, Tokuuye K. Technical considerations for noncoplanar proton-beam therapy of patients with tumors proximal

to the optic nerve. Strahlentherapie und Onkologie : Organ der Deutschen Rontgengesellschaft ... [et al] 2010;186: 36-39.

12. Hata M, Tokuuye K, Sugahara S, Tohno E, Fukumitsu N, Hashimoto T, Ohnishi K, Nemoto K, Ohara K, Sakae T, Akine Y. Proton irradiation in a single fraction for hepatocellular carcinoma patients with uncontrollable ascites. Technical considerations and results. Strahlentherapie und Onkologie : Organ der Deutschen Rontgengesellschaft ... [et al] 2007;183: 411-416.

13. Hata M, Tokuuye K, Sugahara S, Fukumitsu N, Hashimoto T, Ohnishi K, Nemoto K, Ohara K, Matsuzaki Y, Akine Y. Proton beam therapy for hepatocellular carcinoma patients with severe cirrhosis. Strahlentherapie und Onkologie : Organ der Deutschen Rontgengesellschaft ... [et al] 2006;182: 713-720.

14. Cox JD, Stetz J, Pajak TF. Toxicity criteria of the Radiation Therapy

Oncology Group (RTOG) and the European Organization for Research and Treatment of Cancer (EORTC). Int J Radiat Oncol Biol Phys 1995;31: 1341-1346.

15. Nakamura M, Narita Y, Matsuo Y, Narabayashi M, Nakata M, Yano S, Miyabe Y, Matsugi K, Sawada A, Norihisa Y, Mizowaki T, Nagata Y, Hiraoka M. Geometrical differences in target volumes between slow CT and 4D CT imaging in stereotactic body radiotherapy for lung tumors in the upper and middle lobe. Med Phys 2008;35: 4142-4148.

16. Fukumitsu N, Hashimoto T, Okumura T, Mizumoto M, Tohno E, Fukuda K, Abei M, Sakae T, Sakurai H. Investigation of the Geometric Accuracy of Proton Beam Irradiation in the Liver. Int J Radiat Oncol Biol Phys 2011.

17. Seppenwoolde Y, Shirato H, Kitamura K, Shimizu S, van Herk M,

Lebesque JV, Miyasaka K. Precise and real-time measurement of 3D tumor motion in lung due to breathing and heartbeat, measured during radiotherapy. Int J Radiat Oncol Biol Phys 2002;53: 822-834.

18. Onimaru R, Shirato H, Fujino M, Suzuki K, Yamazaki K, Nishimura M, Dosaka-Akita H, Miyasaka K. The effect of tumor location and respiratory function on tumor movement estimated by real-time tracking radiotherapy (RTRT) system. Int J Radiat Oncol Biol Phys 2005;63: 164-169.

19. Nakayama H, Sugahara S, Tokita M, Satoh H, Tsuboi K, Ishikawa S, Tokuuye K. Proton beam therapy for patients with medically inoperable stage I non-small-cell lung cancer at the university of tsukuba. Int J Radiat Oncol Biol Phys 2010;78: 467-471.

20. Nakayama H, Satoh H, Sugahara S, Kurishima K, Tsuboi K, Sakurai H, Ishikawa S, Tokuuye K. Proton Beam Therapy of Stage II and III

Non-Small-Cell Lung Cancer. Int J Radiat Oncol Biol Phys 2010.

21. Shimizu M, Sasaki R, Miyawaki D, Nishimura H, Demizu Y, Akagi T, Suga D, Sakamoto H, Murakami M, Sugimura K, Hishikawa Y. Physiologic reactions after proton beam therapy in patients with prostate cancer: significance of urinary autoactivation. Int J Radiat Oncol Biol Phys 2009;75: 580-586.

Figure legends

Figure 1

Time chart of respiratory-gated Proton beam therapy.

(a) Respiratory waveform.

(b) Threshold level of gating.

(c) Timing of proton beam exposure.

(d) Gate signal.

The proton beam is delivered 0.3 seconds after the waveform drops below the threshold for 0.3 seconds.

Figure 2

A 76-year-old man with lung cancer in the left lung. The images show the CT (pre) (top), registered CT (post) (middle), and dose distribution (bottom). Each image shows the axial, coronal, and sagittal views from left

to right. Fibrosis was located surrounding the tumor. The 90% confidence intervals of the percent normalization of the beam cycle (90% B.C.) value was 7.09%.

Figure 3

A 46-year-old woman with a metastatic lung tumor in the right lung. The fibrosis was located on the antero-medial side of the tumor. The 90% B.C. value was 44.38%.

Fig 1

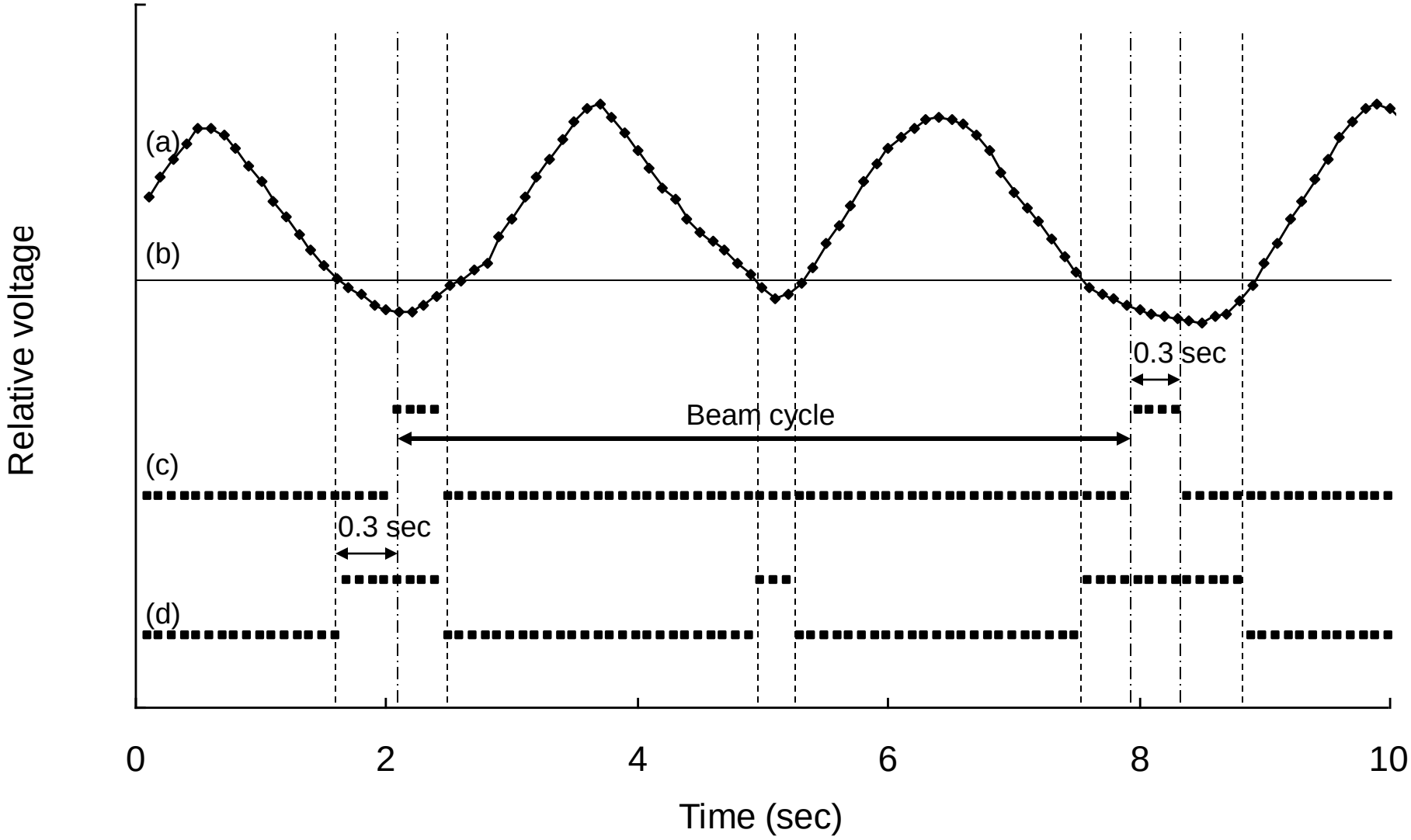
Relative voltage
(a)
(b)
0.3 sec
Beam cycle
(c)
0.3 sec
(d)
0
2
4
6
8
10
Time (sec)

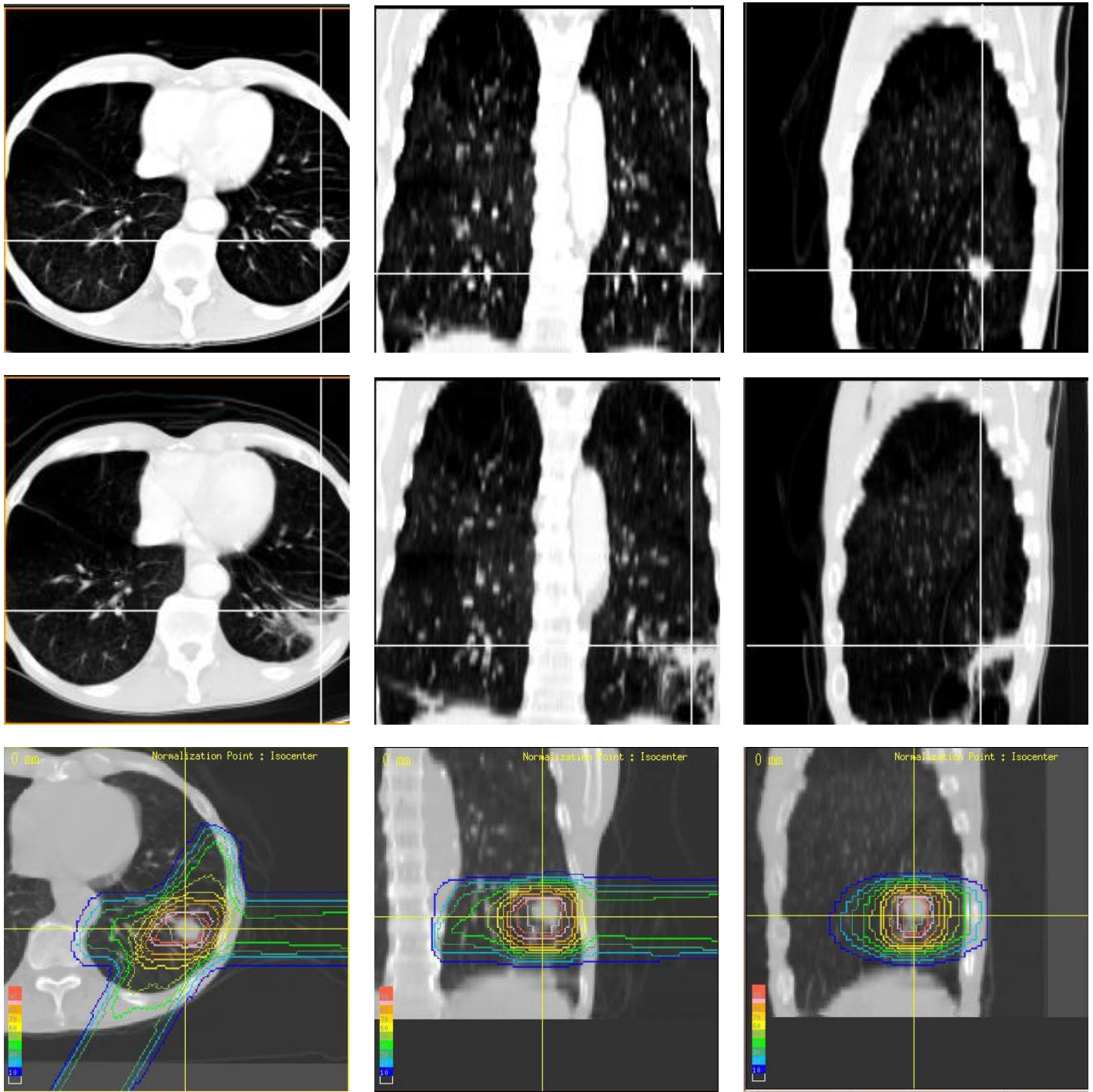
Normalization Point : Isocenter
Normalization Point : Isocenter
Normalization Point : Isocenter

Fig 2

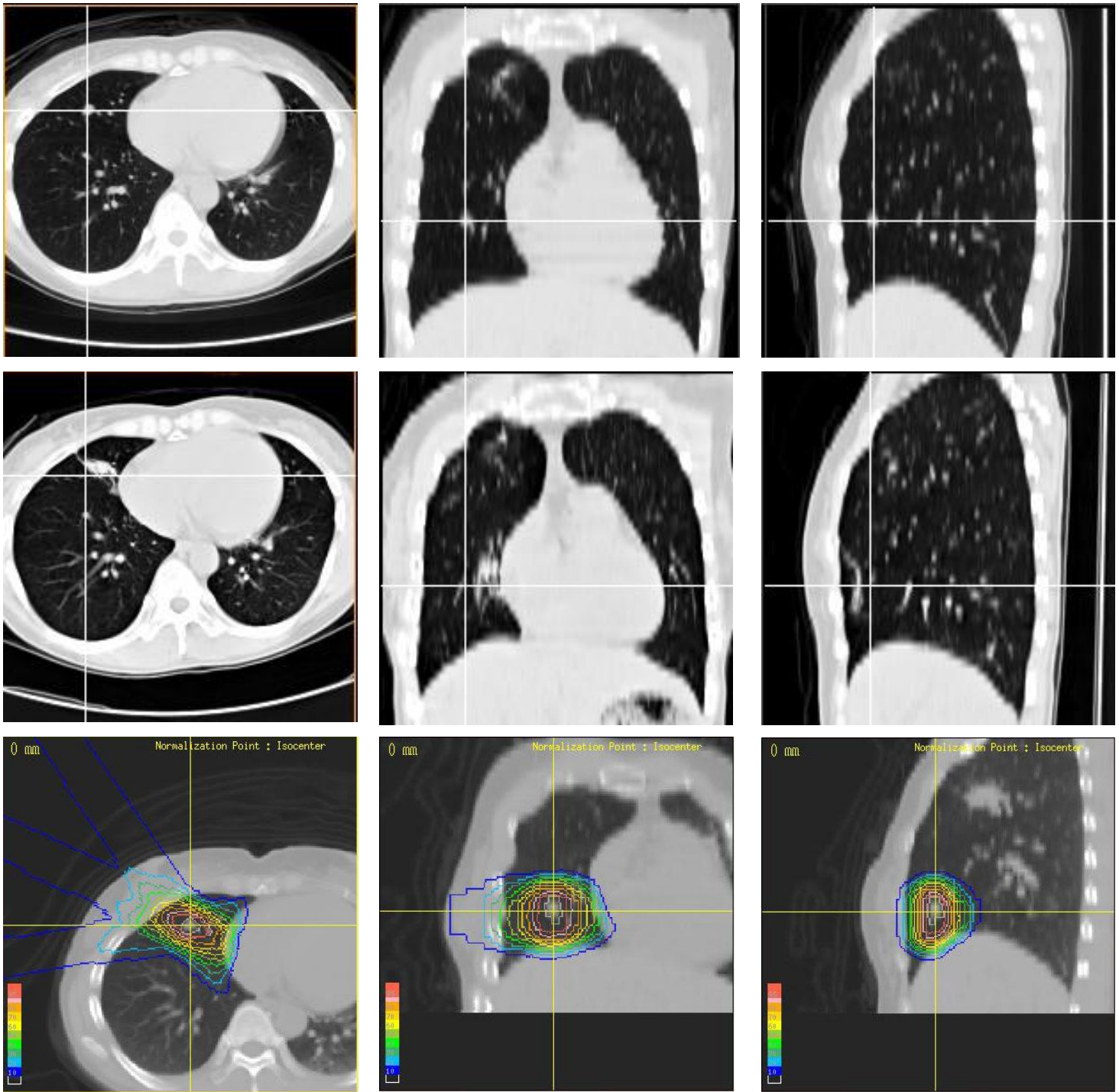
0 mm
Normalization Point : Isocenter
0 mm
Normalization Point : Isocenter
0 mm
Normalization Point : Isocenter

Fig 3

Table 1 Tumor and fibrosis consistency in each classification

		Group A	Group B	P value
90% B.C.	≤ 25%	16	0	0.037 (n=25)
	> 25%	6	3	
Tumor volume	≤ 20cm^3	24	3	> 0.999 (n=50)
	> 20cm^3	21	2	
Tumor location	upper	25	3	> 0.999 (n=50)
	lower	20	2	
Tumor fixation	fix	10	0	0.569 (n= 50)
	free	35	5	
Beam direction	anterior	13	2	0.600 (n= 31)
	posterior	15	1	

Group A: fibrosis overlap with the tumor

Group B: fibrosis not overlap with the tumor